YUCCA MOUNTAIN 2008 PERFORMANCE ASSESSMENT: INCORPORATION OF SEISMIC HAZARD CURVE UNCERTAINTY

Jon C. Helton, Cédric J. Sallaberry

Sandia National Laboratories, Albuquerque, NM 87185-0748, jchelto@sandia.gov

The possible effects of epistemic uncertainty in the seismic hazard curve used in the 2008 performance assessment (PA) for the proposed repository for high-level radioactive waste at Yucca Mountain (YM), Nevada, are investigated. The analysis establishes that it is possible to propagate epistemic uncertainty in the seismic hazard through the computational structure used in the 2008 YM PA and to investigate the effects of this uncertainty on expected dose to a reasonably maximally exposed individual from seismic ground motion events with sensitivity analysis procedures based on Latin hypercube sampling, partial rank correlation, and stepwise rank regression. The dominant analysis inputs affecting the epistemic uncertainty in the indicated dose were found to be the residual stress level at which stress corrosion initiates in the Alloy 22 outer corrosion barrier for waste packages and the seismic hazard curve.

I. INTRODUCTION

Extensive work has been carried out by the U.S. Department of Energy (DOE) in the development of a geologic repository at Yucca Mountain (YM), Nevada, for the disposal of high-level radioactive waste [1-6]. As part of this development, a detailed performance assessment (PA) for the YM repository was completed in 2008 [6] and supported a license application by the DOE to the U.S. Nuclear Regulatory Commission (NRC) for the construction of the YM repository [7]. A summary of the 2008 YM PA (also called the 2008 Total System Performance Assessment or simply the 2008 TSPA) is available in a sequence of papers presented in a special session of the 2008 International High-Level Radioactive Waste Management Conference [8-14].

The 2008 YM PA considered the following scenario classes: nominal (i.e., undisturbed) conditions, early waste package (WP) failure, early drip shield (DS) failure, seismic ground motion (GM), seismic fault displacement, igneous intrusion, and igneous eruption (see [6], App. J, for detailed information on the definition of scenario classes in the 2008 YM PA). A fundamental part of the 2008 YM PA was the determination and representation of the uncertainty present in the occurrence and resultant consequences associated with individual scenario classes. The uncertainties incorporated into the 2008 YM PA were divided into two classes: (i) aleatory uncertainties, which are related to the probability of scenario occurrence, and (ii) epistemic uncertainties, which are related to a lack of knowledge with respect to the correct value to use for a quantity that is believed, or assumed, to a have a fixed value in the context of a specific analysis ([6], App. J).

Of the many potential scenario consequences analyzed in the 2008 YM PA, the most important from a regulatory perspective was expected dose (mrem/yr) to a reasonably maximally exposed individual (RMEI) ([15]; [6], App. J). Specifically, this dose was required to be less than 15 mrem/yr for the first 10,000 yr after repository closure and to be less than 100 mrem/yr after 10,000 yr but within the period of geologic stability, which was assumed to extend to 1,000,000 yr after repository closure ([16], p. 10829). Further, the NRC specified that the indicated bounds on dose to the RMEI were to apply to mean doses ([16], p. 10829).

For the 2008 YM PA, the mean time-dependent dose to which the NRC bounds applied was interpreted to be an expected (i.e., mean) dose over both aleatory uncertainty and epistemic uncertainty ([15]; [6], App. J). This expected (i.e., mean) dose was calculated by first calculating time-dependent doses over aleatory uncertainty conditional on specific realizations of epistemic uncertainty and then calculating the expected (i.e., mean) values of these doses over epistemic uncertainty ([6], App. J). With respect to terminology, expected dose over aleatory uncertainty is referred to as expected dose; and in consistency with terminology used by the NRC, expected dose over aleatory and epistemic uncertainty is referred to as expected (mean) dose or simply mean dose. In the computational strategy used in the 2008 YM PA, expected and expected (mean) dose were first determined for the individual scenario classes and then added to obtain expected and expected (mean) dose to the RMEI from all sources ([6], App. J; [8,13]).

Inputs to the 2008 YM PA involved in the characterization of aleatory uncertainty included the probability p_{EWP} that a WP will experience an early failure, the probability p_{EDS} that a DS will experience an early failure, the occurrence rate λ_{IG} (yr^{-1}) of igneous intrusive events that intersect the repository, and the hazard curve $\lambda_{GM}(v)$ defining the occurrence rate (yr^{-1}) of seismic ground motion events with peak ground velocities (PGVs) that exceed a PGV of v at the subsurface location of the repository.

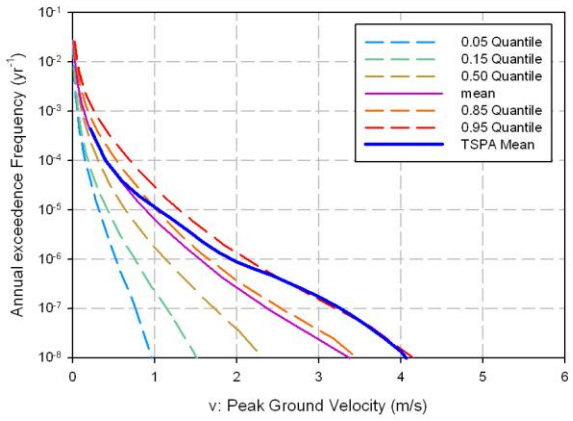

Fig. 1 Quantiles and mean representing uncertainty in seismic hazard curve with mean hazard curve used in 2008 YM PA (i.e., curve labeled TSPA mean).

Epistemic uncertainties in p_{EWP}, p_{EDS} and λ_{IG} were found to be important contributors to the epistemic uncertainty in expected dose to RMEI for the early WP failure, early DS failure, igneous intrusive, and igneous eruptive scenario classes ([6], App. K; [13]) and, as result, significantly affected the expected (mean) doses for these scenario classes. The seismic hazard curve $\lambda_{GM}(v)$ characterizes aleatory uncertainty in the occurrence of seismic GM events that thus plays the same role in the analysis of the seismic GM scenario class as played by p_{EWP}, p_{EDS} and λ_{IG} in the analyses of the early WP failure, early DS failure, igneous intrusive, and igneous eruptive scenario classes. However, although the seismic GM scenario class was an important contributor to expected (mean) dose to the RMEI in the 2008 YM PA, the epistemic uncertainty present in estimates for $\lambda_{GM}(v)$ were not included as part of this PA. The purpose of this presentation is to consider the effects of epistemic uncertainty in the possible values for $\lambda_{GM}(v)$ on expected and expected (mean) dose for the seismic GM scenario class.

II. UNCERTAINTY IN SEISMIC HAZARD CURVE

The seismic hazard curve used in the 2008 YM PA is shown in Fig. 1. Additional potential hazard curves are also shown in Fig. 1 and derive from the uncertainty in exceedance frequencies for individual PGVs. In concept, each labeled quantile curve can be interpreted as a potential hazard curve. The uncertainty in potential hazard curves shown in Fig. 1 was calculated with Approach 3 of Ref. [17] as documented in Ref. [18].

This presentation investigates how the uncertainty in seismic hazard curves shown in Fig. 1 affects the uncertainty in expected dose to the RMEI from seismic GM events. Specifically, results obtained in the 2008 YM PA are recalculated with the seismic hazard curve treated as an epistemically uncertain input to the analysis and with all other analysis assumptions and inputs unchanged from the original 2008 YM PA.

For notational convenience, the hazard curves corresponding to quantiles 0.05, 0.15, 0.5, 0.85 and 0.95 are designated by $\lambda_{GM,1}(v)$, $\lambda_{GM,2}(v)$, $\lambda_{GM,3}(v)$, $\lambda_{GM,4}(v)$ and $\lambda_{GM,5}(v)$, respectively. In consistency with the probabilistic representation of epistemic uncertainty used in the 2008 YM PA, $\lambda_{GM,1}(v)$, $\lambda_{GM,2}(v)$, $\lambda_{GM,3}(v)$, $\lambda_{GM,4}(v)$ and $\lambda_{GM,5}(v)$ are assigned probabilities of 0.1, 0.225, 0.35, 0.225 and 0.1 as indicated in Fig. 2. Further, $\lambda_{GM}(v)$ is used to designate the mean hazard curve used in the 2008 YM PA.

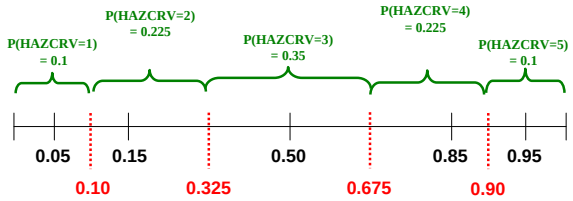

Fig. 2 Probabilistic characterization of epistemic uncertainty in seismic hazard curves.

III. EXPECTED DOSE TO RMEI

A high-level summary of how the seismic hazard curve enters into the determination of expected dose to the RMEI for seismic GM events follows. The presented results are for the first 20,000 yr following repository closure. The 2008 YM PA considered two types of WPs: commercial spent nuclear fuel (CSNF) WPs and codisposed spent fuel (CDSP) WPs. The CSNF WPs are more resistant to seismic GM damage than CSNF WPs and have a very low probability of being damaged by seismic GM events in the first 20,000 yr following repository closure. For this reason, the presented analyses only consider seismic GM damage to CDSP WPs. More detail on the calculation of expected dose from seismic GM events is available in Sect. 6 and App. J of Ref. [6] and in detailed technical reports cited in Ref. [6].

When viewed at a high level, expected dose $\bar{D}_{SG}(\tau \mid \mathbf{e})$ to the RMEI at time τ (yr) for seismic GM events and conditional on the values for epistemically uncertain analysis inputs contained in the vector $\mathbf{e}$ is defined by

$$\begin{aligned}\bar{D}_{SG}(\tau \mid \mathbf{e}) &= \int_0^\tau \lambda_1 \exp(-\lambda_1 t) \\ &\times \left\{ \int_{A_{1,mn}}^{A_{1,mx}} D_{SG}(\tau \mid [t, A], \mathbf{e})\, d_{A1}(A)\, \mathrm{d}A \right. \\ &\left. + \int_t^\tau \left(\int_{A_{2,mn}}^{A_{2,mx}} D_{SG}(\tau \mid [\tilde{t}, A], \mathbf{e})\, d_{A2}(A)\, \mathrm{d}A \right) \lambda_2 \mathrm{d}\tilde{t} \right\} \mathrm{d}t, \end{aligned} \quad (1)$$

where

λ_1 = occurrence rate (yr^{-1}) of seismic GM events that cause damage to CDSP WPs with intact internals,

λ_2 = occurrence rate (yr^{-1}) of seismic GM events that cause damage to CDSP WPs with degraded internals,

$d_{A1}(A)$ = density function (m^{-2}) defined on $[A_{1,mn}, A_{1,mx}]$ for damaged area on a CDSP WP with intact internals conditional on the occurrrence of a damaging seismic GM event,

$d_{A2}(A)$ = density function (m^{-2}) defined on $[A_{2,mn}, A_{2,mx}]$ for damaged area on a CDSP WP with degraded internals conditional on the occurrrence of a damaging seismic GM event,

$D_{SG}(\tau \mid [t, A], \mathbf{e})$ = dose (mrem/yr) to RMEI at time τ that (i) results from a seismic GM event at time t that causes a damaged area A on a CDSP WP and (ii) is conditional on the values for epistemically uncertainty analysis inputs contained in the vector $\mathbf{e}$,

and $D_{SG}(\tau \mid [\tilde{t}, A], \mathbf{e})$ is the same as $D_{SG}(\tau \mid [t, A], \mathbf{e})$ with $t \le \tilde{t}$ and a different density function for A (i.e., $d_{A2}(A)$ rather than $d_{A1}(A)$). Example elements of the vector $\mathbf{e}$ are shown in Table I.

Although not indicated in Eq. (1), λ_1, λ_2, $d_{A1}(A)$ and $d_{A2}(A)$ are functions $\lambda_1(HC, R)$, $\lambda_2(HC, R)$, $d_{A1}(A \mid HC, R, SF)$ and $d_{A2}(A \mid HC, R, SF)$ of epistemically uncertain variables *HC*, *R* and *SF*, where (i) *HC* = *HAZCRV* is a designator for the variable corresponding to the five potential hazard curves and (ii) *R* = *SCCTHRP* and *SF* = *WDCRCDEN* are defined in Table I.

The 2008 YM PA used a Latin hypercube sample (LHS) [19,20] of size 300 in the propagation of epistemic uncertainty. For seismic GM events, the result is a mapping

$$\left[\mathbf{e}_i, \bar{D}_{SG}(\tau \mid \mathbf{e}_i)\right], i = 1, 2, ..., 300, \quad (2)$$

between epistemically uncertain analysis inputs and expected dose from seismic GM events that can be explored with a variety of uncertainty and sensitivity analysis procedures [21]. The analyses contained in this presentation use the same LHS used in the 2008 YM PA with the addition of the pointer variable *HC* = *HAZCRV* to identify the hazard curve associated with each sample element (i.e., $\lambda_{GM,1}(v)$, $\lambda_{GM,2}(v)$, $\lambda_{GM,3}(v)$, $\lambda_{GM,4}(v)$ or $\lambda_{GM,5}(v)$).

Table I Examples of epistemically uncertain variables in the 2008 YM PA that affect dose to the RMEI for seismic GM events (see [6], Tables K3-1, K3-2, K3-3, for additional information)

DSNFMASS. Scale factor used to characterize uncertainty in radionuclide content of defense spent nuclear fuel (dimensionless). *Distribution:* Triangular. *Range:* 0.45 to 2.9. *Mode:* 0.62.
HLWDRACD. Effective rate coefficient (affinity term) for the dissolution of high level waste glass in CDSP WPs under low pH conditions ($g/(m^2d)$). *Distribution:* Triangular. *Range:* 8.41E+03 to 1.15E+07. *Mode:* 8.41E+03.
INFIL. Pointer variable for determining infiltration conditions: 10^{th}, 30^{th}, 50^{th} or 90^{th} percentile infiltration scenario (dimensionless). *Distribution:* Discrete. *Range:* 1 to 4.
MICC14. Groundwater Biosphere Dose Conversion Factor (BDCF) for ^{14}C in modern interglacial climate ($(Sv/year)/(Bq/m^3)$). *Distribution:* Discrete. *Range:* 7.18E-10 to 2.56E-08. *Mean:* 1.93E-09. *Standard Deviation:* 1.85E-09.
MICTC99. Groundwater BDCF for ^{99}Tc in modern interglacial climate ($(Sv/year)/(Bq/m^3)$). *Distribution:* Discrete. *Range:* 5.28E-10 to 2.85E-08. *Mean:* 1.12E-09. *Standard Deviation:* 1.26E-09.
SCCTHRP. Residual stress threshold for stress corrosion cracking nucleation of Alloy 22 (as a percentage of yield strength in MPa) (dimensionless). *Distribution:* Uniform. *Range:* 90 to 105.
SZFIPOVO. Logarithm of flowing interval porosity in volcanic units (dimensionless). *Distribution:* Piecewise uniform. *Range:* -5 to -1. *Mean/Median/Mode:* -3.
SZGWSPDM. Logarithm of scale factor used to characterize uncertainty in groundwater specific discharge (dimensionless). *Distribution:* Piecewise uniform. *Range:* -0.951 to 0.951.
SZKDPUVO. Plutonium sorption coefficient in volcanic units (mL/g). *Distribution:* Piecewise uniform. *Range:* 10 to 300.
THERMCON. Selector variable for one of three host-rock thermal conductivity scenarios (low, mean, and high) (dimensionless). *Distribution:* Discrete. *Range:* 1 to 3.
WDCRCDEN. Ratio of SCC area to unit of seismic damaged area for a waste package (dimensionless). *Distribution:* Uniform. *Range:* 0.00327 to 0.0131.
WDGCUA22. Variable for selecting distribution for general corrosion rate (low, medium, or high) (dimensionless). *Distribution:* Discrete. *Range:* 1 to 3.

IV. UNCERTAINTY ANALYSIS RESULTS

The rates $\lambda_1(HC,R)$ and $\lambda_2(HC,R)$ depend on both the seismic hazard curve (i.e., *HC* = *HAZCRV*) and the residual stress threshold of Alloy 22 (i.e., *R* = *SCCTHRP*) and are potentially important contributors to both the value for $\bar{D}_{SG}(\tau\,|\,\mathbf{e})$ and the epistemic uncertainty associated with this value as a result of their role in the determination of $\bar{D}_{SG}(\tau\,|\,\mathbf{e})$ as indicated in Eq. (1). A comparison of the epistemic uncertainty associated with $\lambda_1(HC,R)$ and $\lambda_2(HC,R)$ with and without the inclusion of hazard curve uncertainty is shown in Fig. 3. As can be seen, the inclusion of hazard curve uncertainty has large effect on $\lambda_2(HC,R)$ and a noticeable but smaller effect on $\lambda_1(HC,R)$.

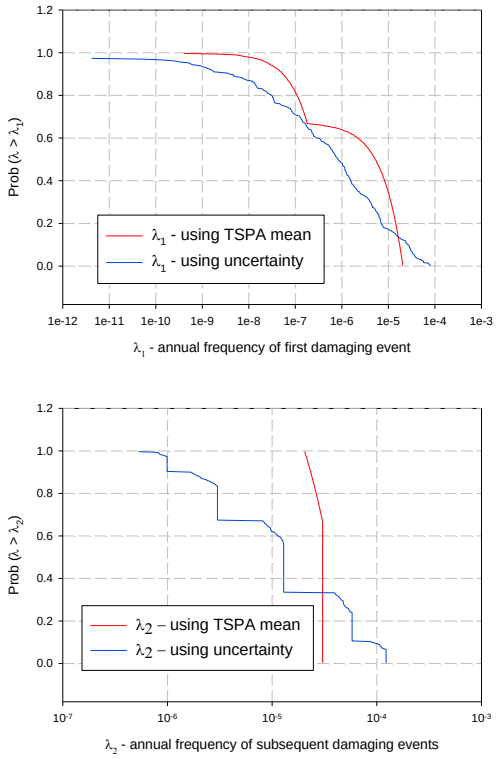

Fig. 3 Comparison of the epistemic uncertainty associated with $\lambda_1(HC,R)$ and $\lambda_2(HC,R)$ with and without the inclusion of hazard curve uncertainty.

In turn, the uncertainty associated with the appropriate value to use for the hazard curve leads to a noticeable spreading in the uncertainty associated with $\bar{D}_{SG}(\tau\,|\,\mathbf{e})$ (Fig. 4). In particular, inclusion of the uncertainty associated with the seismic hazard curve results in more small values for $\bar{D}_{SG}(\tau\,|\,\mathbf{e})$.

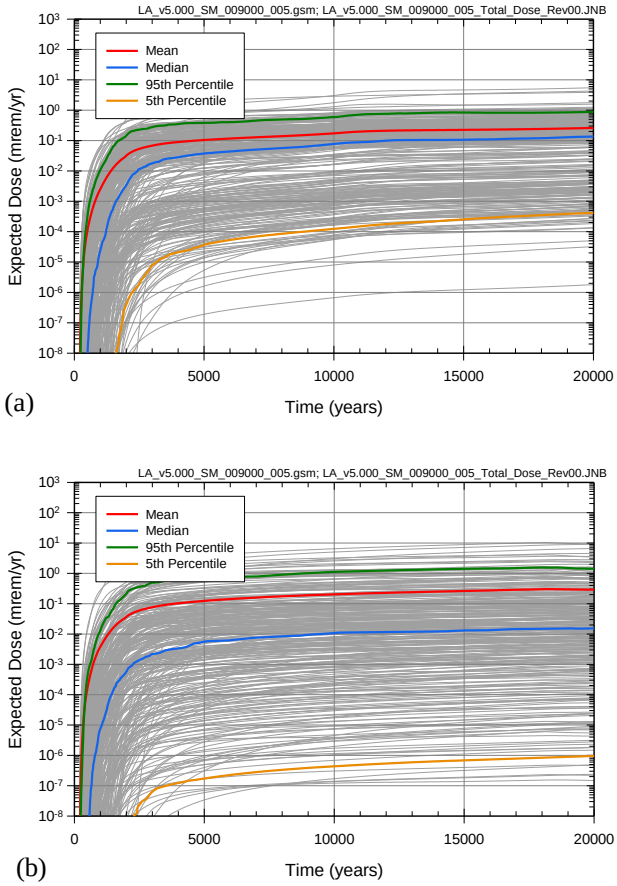

Fig. 4 Comparison of the epistemic uncertainty associated with $\bar{D}_{SG}(\tau\,|\,\mathbf{e})$ without and with the inclusion of hazard curve uncertainty: (a) without, and (b) with.

V. SENSITIVITY ANALYSIS

A comparison of sensitivity analysis results based on partial rank correlation coefficients (PRCCs) for $\bar{D}_{SG}(\tau\,|\,\mathbf{e})$ obtained with and without the inclusion of the uncertainty associated with the seismic hazard curve is presented in Fig. 5 and shows the following: (i) without the inclusion of hazard curve uncertainty, the uncertainty in $\bar{D}_{SG}(\tau\,|\,\mathbf{e})$ is dominated by the uncertainty in the residual stress threshold *R* = *SCCTHRP* for Alloy 22 (Fig. 5a), (ii) with the inclusion of hazard curve uncertainty, the uncertainty in both the hazard curve *HC* = *HAZCRV* and the residual stress threshold *R* = *SCCTHRP* for Alloy 22 are important contributors to the uncertainty in $\bar{D}_{SG}(\tau\,|\,\mathbf{e})$ (Fig. 5b), and (iii) with the inclusion of hazard curve uncertainty, the uncertainty in $\bar{D}_{SG}(\tau\,|\,\mathbf{e})$ is dominated by the uncertainty in the damage rate $\lambda_1(HC,R)$ = *LAMBDA_1* when $\lambda_1(HC,R)$ is included in the analysis instead of *HC* = *HAZCRV* and *R* = *SCCTHRP*

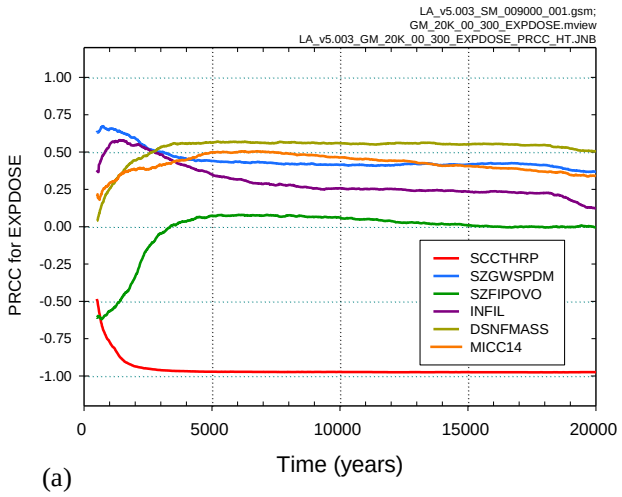

(a)

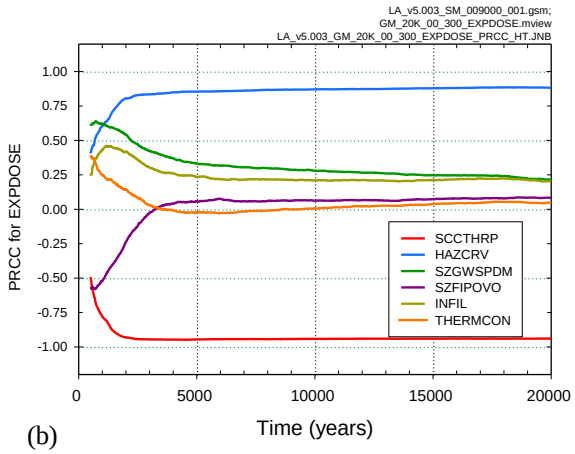

(b)

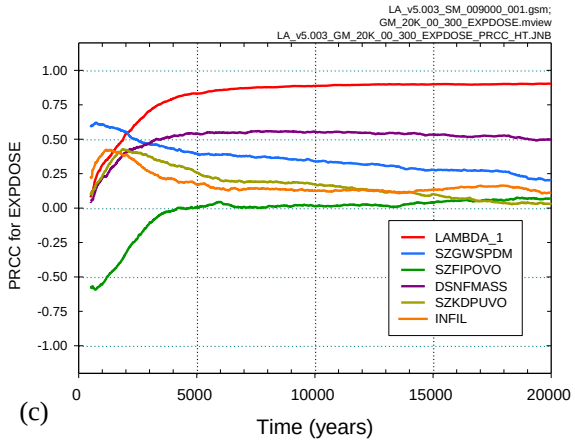

(c)

Fig. 5 Sensitivity analysis results based PRCCs for $\bar{D}_{SG}(\tau \mid \mathbf{e})$ obtained with and without the inclusion of the uncertainty associated with the seismic hazard curve: (a) without hazard curve uncertainty, (b) with hazard curve uncertainty, and (c) with hazard curve uncertainty and $\lambda_1(HC, R)$ = *LAMBDA*_1 replacing *HC* = *HAZCRV* and *R* = *SCCTHRP*.

Table II Stepwise rank regression analyses for $\bar{D}_{SG}(\tau \mid \mathbf{e})$ at 5000 and 10,000 yr: (a) without hazard curve uncertainty, (b) with hazard curve uncertainty, and (c) with hazard curve uncertainty and $\lambda_1(HC, R)$ = *LAMBDA*_1 replacing *HC* = *HAZCRV* and *R* = *SCCTHRP*

(a)	5000 yr			10,000 yr		
Step[α]	**Variable**[β]	**R^2**[γ]	**SRRC**[δ]	**Variable**	**R^2**	**SRRC**
1	**SCCTHRP**	**0.86**	**-0.91**	**SCCTHRP**	**0.88**	**-0.93**
2	MICTC99	0.88	0.10	MICTC99	0.90	0.12
3	DSNFMASS	0.89	0.14	DSNFMASS	0.91	0.14
4	SZGWSPDM	0.90	0.11	HLWDRACD	0.91	0.08
5	MICC14	0.90	0.10	MICC14	0.92	0.08

(b)	5000 yr			10,000 yr		
Step	**Variable**	**R^2**	**SRRC**	**Variable**	**R^2**	**SRRC**
1	**SCCTHRP**	**0.64**	**-0.82**	**SCCTHRP**	**0.61**	**-0.81**
2	**HAZCRV**	**0.88**	**0.49**	**HAZCRV**	**0.89**	**0.53**
3	MICTC99	0.89	0.07	MICTC99	0.90	0.07
4	SZGWSPDM	0.89	0.07	DSNFMASS	0.90	0.07
5	WDGCUA22	0.89	-0.06	WDGCUA22	0.90	-0.06

(c)	5000 yr			10,000 yr		
Step	**Variable**	**R^2**	**SRRC**	**Variable**	**R^2**	**SRRC**
1	**LAMBDA_1**	**0.94**	**0.88**	**LAMBDA_1**	**0.96**	**0.95**
2	MICTC99	0.95	0.07	MICTC99	0.97	0.07
3	SZGWSPDM	0.96	0.06	SZGWSPDM	0.97	0.04
4	SCCTHRP	0.96	-0.10	DSNFMASS	0.98	0.06
5	DSNFMASS	0.96	0.07	HLWDRACD	0.98	0.04

α Steps in stepwise regression analysis with an α-value of 0.01 or less required for a variable to enter a regression model.

β Variables listed in the order of selection in regression analysis.

γ Standardized rank regression coefficients (SRRCs) for variables in final regression model.

δ Cumulative R^2 value with entry of each variable into regression model.

(Fig. 5c). Specifically, $\bar{D}_{SG}(\tau \mid \mathbf{e})$ tends to decrease as *R* = *SCCTHRP* increases as indicated by negative PRCCs in Figs. 5a and 5b and tends to increase as *HC* = *HAZCRV* and $\lambda_1(HC, R)$ increase as indicated by positive PRCCs in Figs. 5b and 5c. A variety of smaller positive and negative effects on $\bar{D}_{SG}(\tau \mid \mathbf{e})$ for other variables are also indicated in Fig. 5 (see Table I for variable definitions).

A more quantitative sensitivity analysis is provided by the stepwise rank regressions in Table II for $\bar{D}_{SG}(\tau \mid \mathbf{e})$ at 5000 and 10,000 yr. The R^2 values in these analyses clearly indicate the dominate effects of the uncertainty in *R* = *SCCTHRP*, *HC* = *HAZCRV* and $\lambda_1(HC, R)$ on $\bar{D}_{SG}(\tau \mid \mathbf{e})$ (i.e., R^2 = 0.86 and 0.88 for *R* = *SCCTHRP* at 5000 and 10,000 yr without the inclusion of hazard curve uncertainty; R^2 = 0.64 and 0.61 for *R* = *SCCTHRP* and R^2

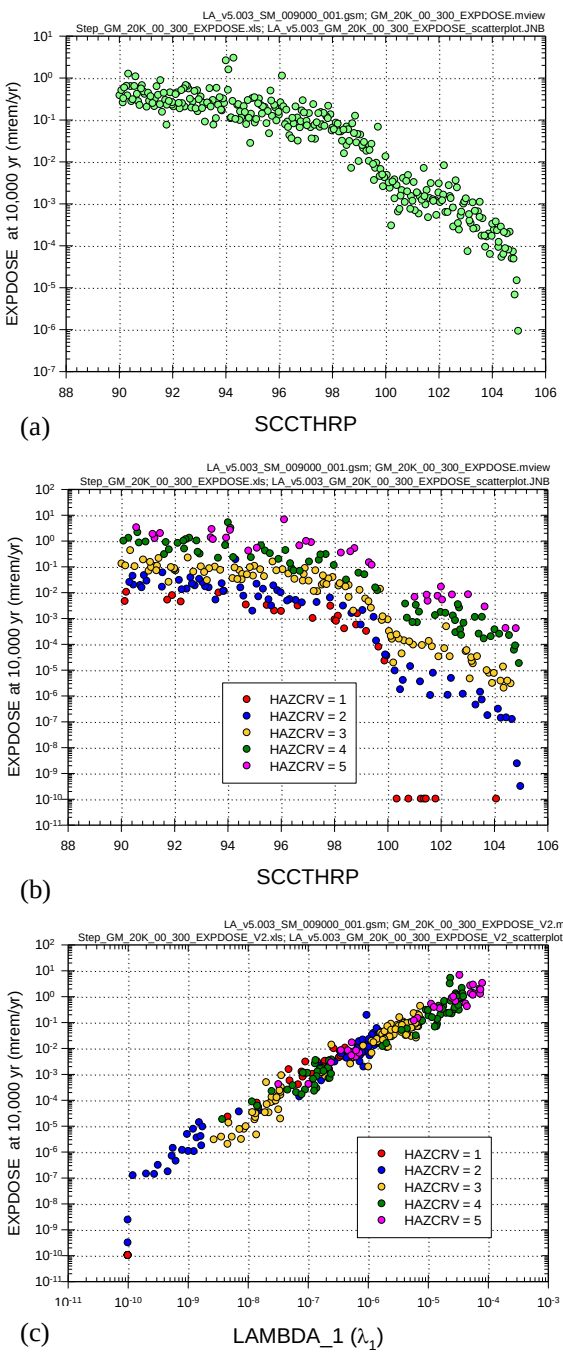

Fig. 6 Scatterplots for R = *SCCTHRP*, HC = *HAZCRV*, $\lambda_1(HC,R)$ = *LAMBDA*_1 and $\bar{D}_{SG}(\tau\,|\,\mathbf{e})$ at 10,000 yr: (a) [$SCCTHRP_i$, $\bar{D}_{SG}(\tau\,|\,\mathbf{e}_i)$], i = 1, 2, …, 300, without inclusion of hazard curve uncertainty, (b) [$SCCTHRP_i$, $\bar{D}_{SG}(\tau\,|\,\mathbf{e}_i)$], i = 1, 2, …, 300, with inclusion of hazard curve uncertainty, and (c) [$LAMBDA\_1_i$, $\bar{D}_{SG}(\tau\,|\,\mathbf{e}_i)$], i = 1, 2, …, 300, with inclusion of hazard curve uncertainty.

= 0. 88 – 0.64 = 0.24 and 0.89 – 0.61 = 0.28 for HC = *HAZCRV* for at 5000 and 10,000 yr with the inclusion of hazard curve uncertainty; and R^2 = 0.94 and 0.95 for $\lambda_1(HC,R)$ = *LAMBDA*_1 at 5000 and 10,000 yr with the inclusion of hazard curve uncertainty).

The sensitivity analyses in based on PRCCs in Fig. 5 and stepwise rank regression in Table II clearly show the dominate effects of R = *SCCTHRP*, HC = *HAZCRV* and $\lambda_1(HC,R)$ = *LAMBDA*_1 on $\bar{D}_{SG}(\tau\,|\,\mathbf{e})$. Additional insights on these effects can be obtained by examining scatterplots involving these variables (Fig. 6). Specifically, the dominant effect of R = *SCCTHRP* on $\bar{D}_{SG}(\tau\,|\,\mathbf{e})$ without the inclusion of hazard curve uncertainty can be seen in Fig. 6a; the combined effect of R = *SCCTHRP* and the inclusion of hazard curve uncertainty on $\bar{D}_{SG}(\tau\,|\,\mathbf{e})$ can be seen in Fig. 6b; and the effect of $\lambda_1(HC,R)$ = *LAMBDA*_1, which incorporates the effects of R = *SCCTHRP* and the inclusion of hazard curve uncertainty into a single variable, on $\bar{D}_{SG}(\tau\,|\,\mathbf{e})$ can be seen in Fig. 6c.

Scatterplots can also be used to examine the relationships between $\lambda_1(HC,R)$ = *LAMBDA*_1, $\lambda_2(HC,R)$ = *LAMBDA*_2, R = *SCCTHRP*, and HC = *HAZCRV* (Fig. 7). The pattern of $\lambda_1(HC,R)$ = *LAMBDA*_1 increasing with increasing values for HC = *HAZCRV* and decreasing with increasing values for R = *SCCTHRP* can be seen in Fig. 7a. A similar, but less pronounced, pattern exists for $\lambda_2(HC,R)$ = *LAMBDA*_2, R = *SCCTHRP* and HC = *HAZCRV* (Fig. 7b). The constant values for $\lambda_2(HC,R)$ when *SCCTHRP* is less than 100 results from the assumption that the probability that WPs with degraded internals will experience an additional failure is the same for all values of *SCCTHRP* less than 100 (see [22], Table 6-77). Finally, the relationship between $\lambda_1(HC,R)$ = *LAMBDA*_1 and $\lambda_2(HC,R)$ = *LAMBDA*_2 can be seen in Fig. 7c, with $\lambda_2(HC,R)$ increasing as $\lambda_1(HC,R)$ increases due to the effect of HC = *HAZCRV* and then leveling off due to the effect of R = *SCCTHRP*.

VI. SUMMARY

The capability to propagate the epistemic uncertainty present in estimates for the seismic hazard curve within the uncertainty structure employed in the 2008 YM PA is demonstrated. This demonstration establishes that it is possible to treat epistemic uncertainty in the definition of the seismic hazard curve in a manner that is conceptually consistent with the manner in which the epistemic uncertainties in the probability p_{EWP} that a WP will experience an early failure, the probability p_{EDS} that a DS

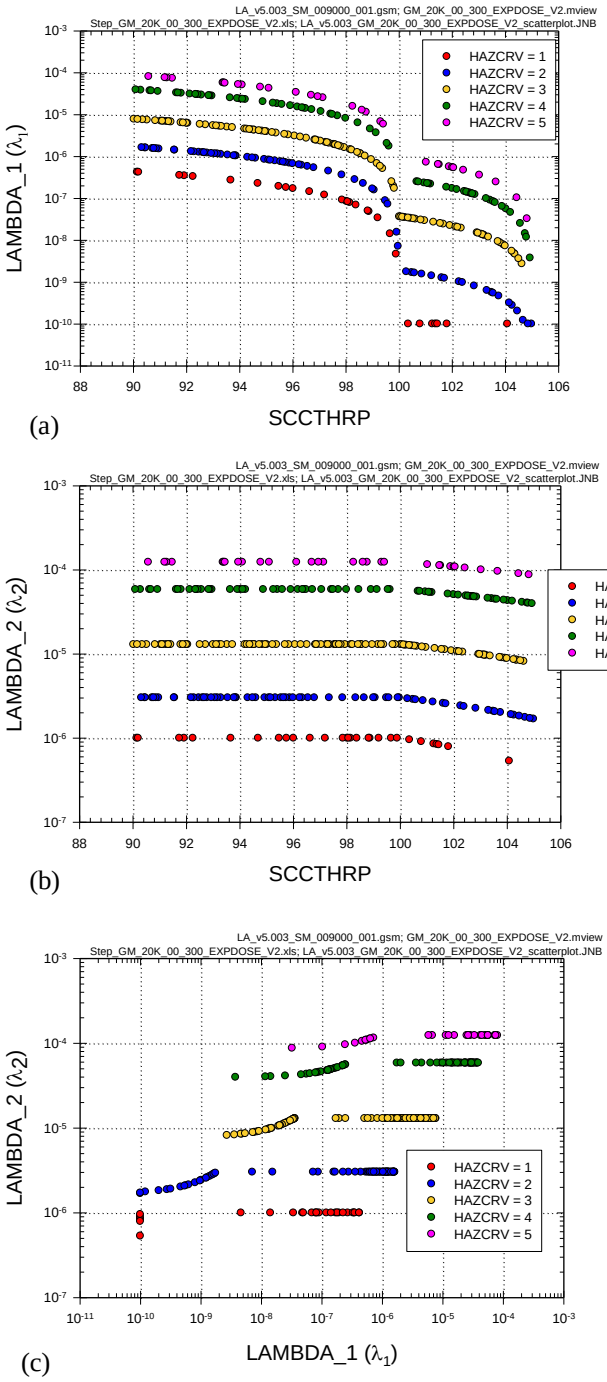

Fig. 7 Scatterplots for $\lambda_1(HC, R)$ = *LAMBDA*_1, $\lambda_2(HC, R)$ = *LAMBDA*_2, R = *SCCTHRP*, and HC = *HAZCRV* : (a) [*SCCTHRP*$_i$, *LAMBDA*_1$_i$], i = 1, 2, …, 300, (b) [*SCCTHRP*$_i$, *LAMBDA*_2$_i$], i = 1, 2, …, 300,, and (c) [*LAMDA*_1$_i$, *LAMBDA*_2$_i$], i = 1, 2, …, 300.

will experience an early failure, and the occurrence rate λ_{IG} (yr^{-1}) of igneous intrusive events that intersect the repository were treated in the 2008 YM PA.

The presented uncertainty and sensitivity studies indicate that the epistemic uncertainty present in estimates of expected dose $\bar{D}_{SG}(\tau \mid \mathbf{e})$ to the RMEI from seismic GM events is dominated by the epistemic uncertainty present in estimates for (i) the residual failure stress *SCCTHRP* for Alloy 22 and (ii) the seismic hazard curve. Given the structure of the 2008 YM PA and the uncertainty in the seismic hazard curve assumed in this analysis, *SCCTHRP* has a somewhat greater effect on the uncertainty in estimates for $\bar{D}_{SG}(\tau \mid \mathbf{e})$ than the seismic hazard curve. However, changes in the uncertainty characterizations for either *SCCTHRP* or the seismic hazard curve could change this ordering.

In this analysis, the primary effect of including the uncertainty in the seismic hazard curve was to expand the range of possible values for $\bar{D}_{SG}(\tau \mid \mathbf{e})$. In particular, more small values for $\bar{D}_{SG}(\tau \mid \mathbf{e})$ were observed than in the original analysis for $\bar{D}_{SG}(\tau \mid \mathbf{e})$ in the 2008 YM PA. However, the expected value $\bar{\bar{D}}_{SG}(\tau \mid \mathbf{e})$ for expected value for dose to the RMEI over both aleatory and epistemic uncertainty obtained in this study is similar to the value for $\bar{\bar{D}}_{SG}(\tau \mid \mathbf{e})$ obtained in the 2008 YM PA.

ACKNOWLEDGMENTS

Work performed at Sandia National Laboratories (SNL), which is a multiprogram laboratory operated by Sandia Corporation, a Lockheed Martin Company, for the U.S. Department of Energy's National Nuclear Security Administration under Contract No. DE-AC04-94AL85000.

REFERENCES

1. U.S. DOE (U.S. Department Of Energy). *Final Environmental Impact Statement for a Geologic Repository for the Disposal of Spent Nuclear Fuel and High-Level Radioactive Waste at Yucca Mountain, Nye County, Nevada*.DOE/EIS-0250F.Washington, D.C.: U.S. Department of Energy, Office of Civilian Radioactive Waste Management 2002.
2. U.S. DOE (U.S. Department Of Energy). *Yucca Mountain Science and Engineering Report, Rev. 1*.DOE/RW-05391.Washington, D.C.: U.S. Department of Energy, Office of Civilian Radioactive Waste Management 2002.
3. CRWMS M&O (Civilian Radioactive Waste Management System Management And Operating Contractor). *Total System Performance Assessment for the Site Recommendation*.TDR-WIS-PA-000001 REV 00.Las Vegas, NV: CRWMS M&O 2000.

4. U.S. DOE (U.S. Department Of Energy). *Viability Assessment of a Repository at Yucca Mountain*.DOE/RW-0508.Washington, D.C.: U.S. Department of Energy, Office of Civilian Radioactive Waste Management 1998.
5. USGS (U.S. Geological Survey). *Yucca Mountain as a Radioactive Waste Repository*. Circular 1184. Denver, CO: USGS Information Services 1999.
6. SNL (Sandia National Laboratories). *Total System Performance Assessment Model/Analysis for the License Application*.MDL-WIS-PA-000005 Rev 00, AD 01.Las Vegas, NV: U.S. Department of Energy Office of Civilian Radioactive Waste Management 2008.
7. U.S. DOE (U.S. Department Of Energy). *Yucca Mountain Repository License Application*. DOE/RW-0573, Rev. 0.Las Vegas, NV: U. S. Department of Energy 2008.
8. HELTON JC et al. Yucca Mountain 2008 Performance Assessment: Conceptual Structure and Computational Implementation. In. *Proceedings of the International High-Level Radioactive Waste Management Conference, September 7-11, 2008*: American Nuclear Society, 2008:524-532.
9. MACKINNON RJ et al. Yucca Mountain 2008 Performance Assessment: Modeling the Engineered Barrier System. In. *Proceedings of the 2008 International High-Level Radioactive Waste Management Conference, September 7-11, 2008*: American Nuclear Society, 2008:542-548.
10. MATTIE PD et al. Yucca Mountain 2008 Performance Assessment: Modeling the Natural System. In. *Proceedings of the 2008 International High-Level Radioactive Waste Management Conference, September 7-11, 2008*: American Nuclear Society, 2008:550-558.
11. SEVOUGIAN SD et al. Yucca Mountain 2008 Performance Assessment: Modeling Disruptive Events and Early Failures. In. *Proceedings of the 2008 International High-Level Radioactive Waste Management Conference, September 7-11, 2008*: American Nuclear Society, 2008:533-541.
12. SALLABERRY CJ et al. Yucca Mountain 2008 Performance Assessment: Uncertainty and Sensitivity Analysis for Physical Processes. In. *Proceedings of the 2008 International High-Level Radioactive Waste Management Conference, September 7-11, 2008*: American Nuclear Society, 2008:559-566.
13. HANSEN CW et al. Yucca Mountain 2008 Performance Assessment: Uncertainty and Sensitivity Analysis for Expected Dose. In. *Proceedings of the 2008 International High-Level Radioactive Waste Management Conference, September 7-11, 2008*: American Nuclear Society, 2008:567-574.
14. SWIFT PN et al. Yucca Mountain 2008 Performance Assessment: Summary. In. *Proceedings of the 2008 International High-Level Radioactive Waste Management Conference, September 7-11, 2008*: American Nuclear Society, 2008:575-581.
15. HELTON JC, SALLABERRY CJ. Conceptual Basis for the Definition and Calculation of Expected Dose in Performance Assessments for the Proposed High-Level Radioactive Waste Repository at Yucca Mountain, Nevada. *Reliability Engineering and System Safety* 2009;94:677-698.
16. U.S. NRC (U.S. Nuclear Regulatory Commission). 10 CFR Part 63: Implementation of a Dose Standard after 10,000 Years. *Federal Register* 2009;74(48):10811-10830.
17. U. S. NRC (U.S. Nuclear Regulatory Commission). *Technical Basis for Revision of Regulatory Guidance on Design Ground Motions: Hazard- and Risk-Consistent Ground Motion Spectra*.NUREG/CR-6728.Washington, DC: United States Nuclear Regulatory Commission 2001.
18. SNL (Sandia National Laboratories). *Supplemental Earthquake Ground Motion Input for a Geologic Repository at Yucca Mountain, NV*.MDL-MGR-GS-000007 REV 00.Las Vegas, NV: Sandia National Laboratories 2008.
19. MCKAY MD et al. A Comparison of Three Methods for Selecting Values of Input Variables in the Analysis of Output from a Computer Code. *Technometrics* 1979;21(2):239-245.
20. HELTON JC, DAVIS FJ. Latin Hypercube Sampling and the Propagation of Uncertainty in Analyses of Complex Systems. *Reliability Engineering and System Safety* 2003;81(1):23-69.
21. HELTON JC et al. Survey of Sampling-Based Methods for Uncertainty and Sensitivity Analysis. *Reliability Engineering and System Safety* 2006;91(10-11):1175-1209.
22. SNL (Sandia National Laboratories). *Seismic Consequence Abstraction*.MDL-WIS-PA-000003 REV 03. Las Vegas, NV: Sandia National Laboratories 2007.